Multiple spin-glass-like behaviors in a Pr-based bulk metallic glass

Yong Tian Wang, Hai Yang Bai, Ming Xiang Pan, De Qian Zhao, and Wei Hua Wang*
Institute of Physics, Chinese Academy of Sciences, Beijing 100080, China
(Received 19 March 2006; revised manuscript received 10 May 2006; published 25 August 2006)

Multiple spin-glass-like (SGL) behaviors have been observed in a $Pr_{60}Al_{10}Ni_{10}Cu_{16}Fe_4$ bulk metallic glass (BMG). Various measurements are carried out to confirm the coexistence of a reentrant-SGL ordering at 14 K, and two cluster-SGL transitions around 6 K and 280 K. The unusual multiple SGL behaviors are ascribed to the couple between the magnetic nanoclusters and the amorphous matrix. The combination of the intrinsic inhomogeneity, spontaneous nanoconfinement and magnetic completing in the BMG leads to the three qualitatively distinct SGL transitions with unique characteristics such as the elevated freezing temperature close to room temperature in cluster SGL. Comparing with the most spin glass (SG) materials with only one SG phase, the Pr-based BMG with multiple SGL phases provides an ideal prototype to fill up the gap for the unknown interactions between two or more SGs, which is of significance to expand current understanding of both SG and more complex systems.

DOI: 10.1103/PhysRevB.74.064422 PACS number(s): 61.43.Fs, 61.25.Mv, 81.05.Kf

I. INTRODUCTION

For the last several decades, spin-glass (SG) has been extensively studied as a prototype of complex systems, and the SG theory has already found applications to several fields outside its original scope, such as combinatorial optimization, categorization theory, associative memories and information theory.[1–3] The SG was originally coined to describe some magnetic alloys in which there was observed orientations' freezing of the magnetic moments (spins). The attempt to understand the cooperative physics of such alloys has exposed many previously unknown and unanticipated fundamental concepts and led to the devising of new analytical, experimental and computer simulation techniques.[1] Therefore, a large number of SG materials have been widely found, and so far there are three main kinds of SGs including surface SG,[4–7] reentrant SG,[8–10] and cluster SG,[11,12] which have been intensively studied in nanoparticle systems, single crystals and polycrystalline materials. However, to the best of our knowledge, the most conventional SG materials contain only one SG phase, and the intricate interactions between two or more SGs remain a major mystery. Accordingly, a sample with intrinsic multiple SG transitions is highly desirable and its availability is closely associated with the prototype for multiple complex systems. These have had major ramifications throughout the whole study of problems involving assemblies of strongly interacting individual entities in which competitive forces yield complex cooperative behavior.[1–3,13] In addition, the most SG transitions in conventional nanoparticle and crystal systems occur in rather low temperature, few SGs freezing near room temperature (RT) have been reported, while such SGs can advantage the fine tuning of freezing state through more available external operations such as light perturbation.[14]

In this work, the unusual multiple SGL behaviors have been observed in a $Pr_{60}Al_{10}Ni_{10}Cu_{16}Fe_4$ bulk metallic glass (BMG) with the intrinsic disordered microstructure and unique characteristics that are markedly different from that of the nanoparticle and the crystal materials.[15] The multiple SGL phases comprise a reentrant-SGL ordering at 14 K (i.e., paramagnetic to ferromagnetic state at 17 K, and then ferromagnetic to SGL state at 14 K), and two cluster-SGL transitions around 6 K and 280 K. In order to understand the multiple SGL behaviors, we have systematically measured the properties of the Pr-based BMG including the T dependence of ac and dc susceptibility at different frequencies and magnetic fields, the magnetization and magnetic relaxation at different temperatures, the electronic resistivity, and magnetic domains. The multiple SGL behaviors are ascribed to the intrinsic inhomogeneity and spontaneous nanoscale confinement within the BMG, which provides an attractive platform for modeling more complex collective phenomena in a broad variety of systems such as SGs, ferrofluids, and dense colloidal suspensions.

II. EXPERIMENTAL

$Pr_{60}Al_{10}Ni_{10}Cu_{16}Fe_4$ alloy was prepared by arc melting pure Pr, Al, Ni, Cu, and Fe in an argon atmosphere. The ingots were remelted and suck cast into a Cu mold under argon atmosphere to get a cylindrical rod of 5 mm in diameter. The amorphous nature of the as-cast alloys was ascertained by x-ray diffraction (XRD) using a MAC M03 XHF diffractometer with Cu $K\alpha$ radiation. Thermal analysis was carried out in a Perkin-Elmer DSC-7 differential scanning calorimeter under a continuous argon flow at a heating rate of 20 K/min. The magnetism and four-point electrical resistance measurements were performed using a PPMS 6000 of Quantum Design Company with high accuracy of 10^{-6} emu and 10^{-4} Ω, respectively. The study of domain structure was carried out by using Digital Instruments NanoScope III a D-3000 MFM. The acoustic velocities of the specimens at room temperature were measured using a pulse-echo overlap technique. The travel time of ultrasonic waves propagating through the specimen with a 10 MHz frequency was measured using a MATEC 6600 ultrasonic system with a measuring sensitivity of 0.5 ns. Elastic constants and the Debye temperature θ_D of the alloys were obtained from the acoustic velocities and the densities.[16]

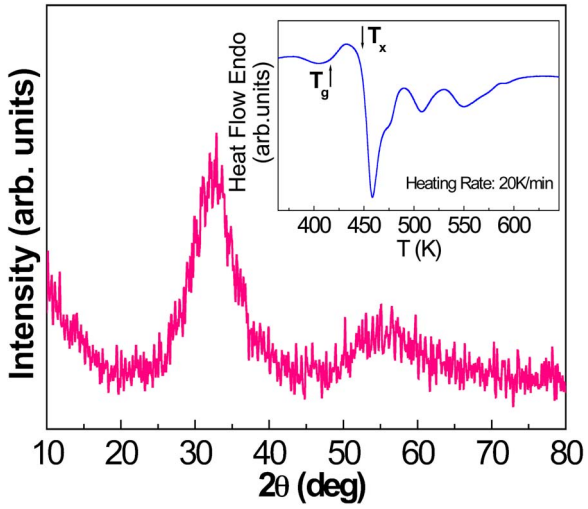

FIG. 1. (Color online) XRD pattern of the as-cast $Pr_{60}Al_{10}Ni_{10}Cu_{16}Fe_4$ BMG. The insert shows the DSC trace of the BMG.

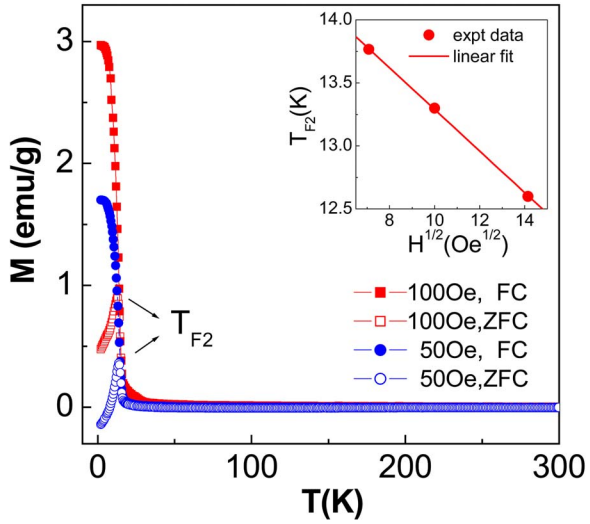

FIG. 2. (Color online) FC and ZFC magnetization measured at different fields. The insert shows the field dependence of the freezing temperatures, plotted as T_{F2} vs $H^{1/2}$.

III. RESULTS

Figure 1 shows the XRD pattern of the as-cast $Pr_{60}Al_{10}Ni_{10}Cu_{16}Fe_4$ alloy. Two broad diffraction peaks indicating amorphous structure and no appreciable diffraction peaks corresponding to crystalline phase are seen for the sample within the resolution limit of the XRD. The insert of Fig. 1 shows the DSC trace of the BMG. The crystallization process includes three exothermic reactions showing the stepwise transformation from the glass into the crystalline state. The remarkable feature of the DSC trace is an obvious endothermic characteristic before crystallization indicating a glass transition at 423 K. The first crystallization event occurs at $T_{x1}=455$ K. The supercooled liquid region or softening region, $\Delta T=T_{x1}-T_g=32$ K. The liquidous temperature T_l of the alloys is 737 K. The distinct glass transition, sharp crystallization events further confirm the amorphous state of the alloy. The Young's modulus E, shear modulus G, bulk modulus K, Poisson's ratio ν, and the Debye temperature θ_D of the alloys determined from the acoustic velocities are 38.06 GPa, 14.09 GPa, 42.56 GPa, 0.351, 163 K, respectively. The fragility m (m is an index of how fast the viscosity increases while approaching the structural arrest at T_g) of the Pr-based alloy, is about 31.[17]

The zero field cooled (ZFC) and field cooled (FC) magnetization curves of the BMG are shown in Fig. 2, and the insert shows the field dependence of the peak temperature T_{F2}. The ZFC and FC branches are measured on warming after initially cooling from 300 to 2 K in zero field and the measuring field, respectively. Low field dc magnetization exhibits the onset of the irreversibility between the ZFC and FC curves around 14 K, which corresponds to the development of a collective frozen magnetic state with the randomly oriented magnetic moments. Above the bifurcation temperature $T_{F2}\approx 14$ K, the ZFC and FC curves coincide; whereas below T_{F2}, they split, and the ZFC branch decreases rapidly while the FC branch increases to a plateau. The sharp maximum in the ZFC curve is broadened and pushed toward lower T with increasing the dc field. These features are typical characteristics of a SG.[12] Further quantitative evidence is given by the Almeida-Thouless (AT) relationship for the most canonical SG systems, which explains the critical lines span with the variable temperature and magnetic field by the mean-field SG model.[5,6,12] The insert of Fig. 2 shows the linear relationship of T_{F2} vs $H^{1/2}$, corresponding to the so-called AT line given by $H_{AT}(T)/\Delta J \propto (1-T/T_F)^{1/2}$, where T_F is the zero-field SG freezing temperature and ΔJ is the width of the distribution of exchange interactions. The linear AT line implies the spin disorder in the whole volume of the BMG, expecting a reentrant SGL behavior at $T_{F2}\approx 14$ K,[5,18] if the spin disorder is limited in the localized layer, e.g., surface-SG, T_F should follow the $H^{3/2}$.[5,6]

Two important features can be found from Fig. 2. One is that the extrapolation of the AT line to $H=0$ gives the SGL transition temperature $T_{F2}\approx 14.5$ K, which is consistent with the observed $M(T)$ at low field. Another is that the extrapolation of the line forward to $T=0$ gives a critical cooling field $H_{cri}\approx 8.2$ kOe, indicating the SGL can disappear when $H > H_{cri}$, which is in perfect agreement with the kink feature around 8 kOe in the following magnetization results at 2 K. The compliance of the data with AT line is considered to be a strong evidence for the existence of a reentrant-SGL phase in the Pr-based BMG.

Nevertheless, a careful analysis of the ZFC and FC branches clearly reveals the coexistence of another slight irreversibility between the ZFC and FC curves around $T_{F3}\approx 250$ K, and a sudden increase in the FC magnetization below $T_{F1}\approx 8$ K (see Fig. 3). The irreversible magnetization near RT is two orders of magnitude lower than that around T_{F2} and the peak is rather broad, indicating some larger spin clusters are slightly frozen (i.e., cluster SGL).[11] The sudden increase of FC magnetization is much clear in the dM/dT plot, which is also one typical characteristics of a freezing process.[5] In other words, some moments can freeze below T_{F1} and align with the direction of external field in the FC process, thus the FC magnetization exhibits a sudden in-

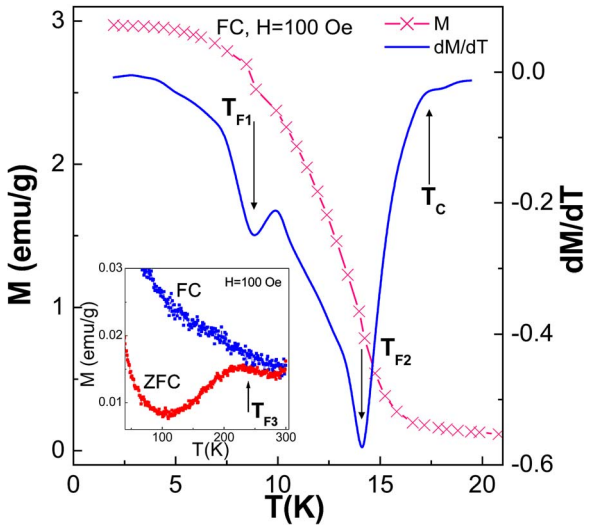

FIG. 3. (Color online) Typical FC curve M (left axis) and dM/dT (right axis) as a function of the temperature measured at 100 Oe. The insert shows the enlarged FC and ZFC branches in high temperature.

crease below T_{F1}. Each forenamed behavior, including reentrant SG and cluster SG, has been separately observed in different nanoparticle or crystal systems, while few materials with two or more SG phases have been reported before.

To verify the coexistence of the three different SGL transitions in the BMG, the T-dependent ac susceptibility is measured at several frequencies ranging from 10 Hz to 10 kHz. The sample is first cooled from RT to 2 K in zero magnetic field, then a probing ac magnetic field of 10 Oe is applied to measure the susceptibility χ as T is slowly raised in short steps to 300 K. Figure 4(a) and 4(b) show the real (χ') and imaginary (χ'') components of the ac susceptibility of the BMG versus T under different frequencies. The insert of Fig. 4(a) shows the T dependent χ' (right axis) and $1/\chi'$ (left axis) at $\omega=1$ kHz, the solid line is the Curie-Weiss fit. According to the Curie-Weiss law:[10] $\chi=C/(T-\theta_w)$, the system undergoes a paramagnetic to ferromagnetic state (PM-FM) at the Curie temperature $T_C\approx 17$ K. With increasing temperature, the magnetization above 100 K gradually deviates the Curie-Weiss behavior, the obvious deviation is due to a magnetic cluster freezing near RT. The χ' curve shows two maxima at $T_{F2}\approx 14$ K and $T_{F3}\approx 280$ K, and a small shoulder around $T_{F1}\approx 6$ K, but the χ'' curve with one order of magnitude smaller than χ' shows three well-defined peaks near T_{F1}, T_{F2}, and T_{F3} [see Figs. 4(a) and 4(b)]. Both χ' and χ'' show evident maxima with amplitudes and positions depending on the frequency ω of the applied ac magnetic field. As frequency is raised the χ' peak amplitudes diminish and all peak temperatures shift linearly to high T with $\ln\omega$ (see Fig. 5), confirming the presence of relaxation processes. The value of frequency sensibility of $T_F(\omega)$, $\delta T_F=\Delta T_F/(T_F\Delta\ln\omega)$, has been used as a possible distinguishing criterion for the presence of a SG phase.[12,18] At T_{F1}, T_{F2}, and T_{F3}, defined by the maximum in χ' at 10 Hz, $\delta T_{F1}=0.005$, $\delta T_{F2}=0.012$, and $\delta T_{F3}=0.01$. For canonical SGs, the δT_F lies between 0.0045 and 0.06, whereas for the known superparamagnetic system it has a value larger than 0.1.[18] All of our values fall into the SG range and the quantitative measurement clearly shows there exist three different SGL phases in the BMG.

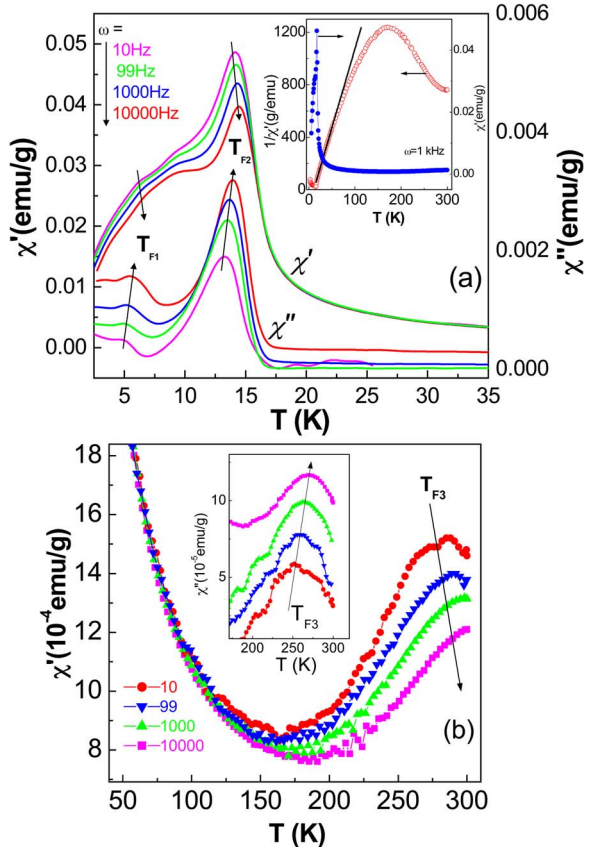

FIG. 4. (Color online) (a) Real (χ') and imaginary (χ'') components of the ac susceptibility of the BMG vs T at frequencies from 10 Hz to 10 kHz in an applied ac field of 10 Oe. The insert shows the temperature dependence of the susceptibility (right axis) and inverse susceptibility (left axis), the solid line is the Curie-Weiss fit. (b) the ac susceptibility in high temperature.

As shown in Fig. 5, the experimental data can be fitted well using the empirical Vogel-Fulcher law:[11,12,18] $\omega=\omega_0\exp[-E_a/k_B(T_F-T_0)]$, with three fitting parameters: characteristic frequency ω_0, activation energy E_a (k_B is the Boltzmann constant), and Vogel-Fulcher temperature T_0, which is a measure of interaction strength. The best fit of this equation to the experimental data yields the values: $\omega_{01}\approx 10^{13}$ Hz, $E_{a1}\approx 31$ K, and $T_{01}=4.5$ K; $\omega_{02}\approx 10^{13}$ Hz, $E_{a2}\approx 40$ K, and $T_{02}=12.6$ K; $\omega_{03}\approx 10^{7}$ Hz, $E_{a3}\approx 275$ K, and $T_{03}=233$ K. For a typical SG system, T_0 is very close to T_F, whereas T_0 is very small compared to T_F in a superparamagnet.[11] Therefore, the closeness of T_0 and T_F further characterizes the three SGL transitions. However, the obtained $\omega_{03}\approx 10^{7}$ Hz suggests a slower spin dynamics near RT compared with ω_{01} and ω_{02} in low T which are 10^{13} Hz typically taken in the most SG systems.[11,12] Combining the much broader peaks in both dc and ac magnetization curves, the SGL features at T_{F3} can be identified as strongly interacted clusters rather than individual spins. In contrast to the conventional cluster-SG freezing below 110 K, even down to 10 K in nanoparticle or

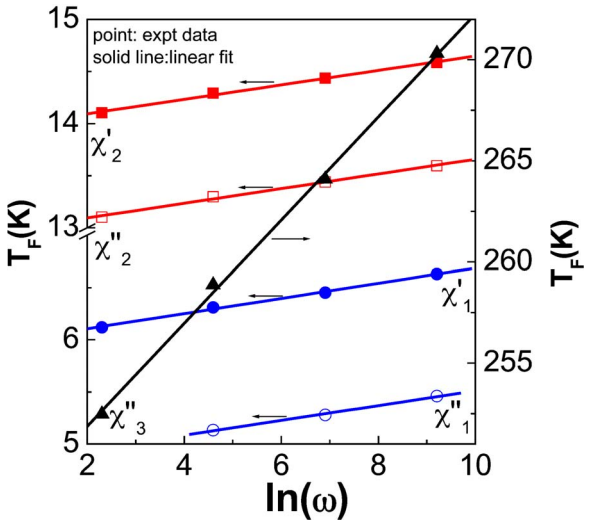

FIG. 5. (Color online) The plot of ac susceptibility peak temperature T_F vs ln ω.

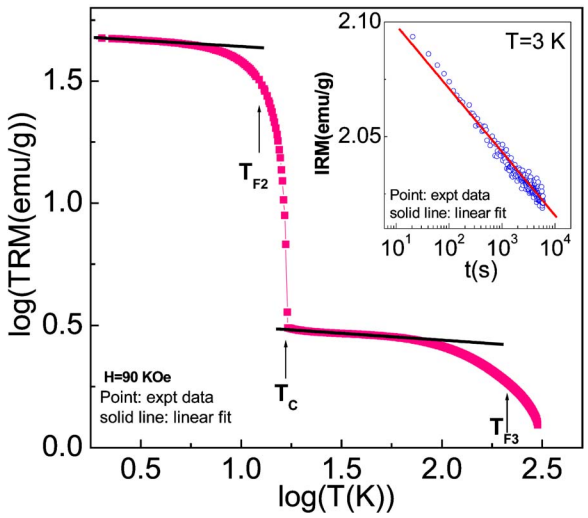

FIG. 7. (Color online) The log-log plot of the thermoremanent magnetization (TRM) versus temperature, the solid line shows the sectional linear fit. The insert shows the time decay of the isothermal remanent magnetization (IRM) at 3 K.

polycrystalline samples,[11,12] the cluster-SGL in the BMG has a greatly elevated freezing temperature close to RT, which can accelerate the magnetic nanoclusters' relaxation and advantage the fine tuning of freezing state through more available external operations such as light perturbation.[14] The magnetization data provides unambiguous evidence for the coexistence of three different SGL phases in the BMG.

The electronic transport measurement can reflect a total picture of the multiple SGL behaviors and show more evidences. Figure 6 shows the T dependence of the electrical resistivity ρ and its derivative $d\rho/dT$, the insert provides more details in a wide temperature range of 2 to 300 K. Two important aspects of the data are noted: First, the BMG exhibits a large residual resistivity $\rho_{rr}=53.8\ \mu\Omega$ cm and a small residual resistivity ratio $\rho_{300\ \mathrm{K}}/\rho_{2\ \mathrm{K}}=1.8$, which are attributed to the scattering of the structural disorder as is usually observed in metallic SGs.[12] Second, almost no anomaly is observed in the $\rho(T)$ curve (see the insert of Fig. 6), indicating no long-range magnetic phase transitions near the three freezing temperatures. It is known that the lack of

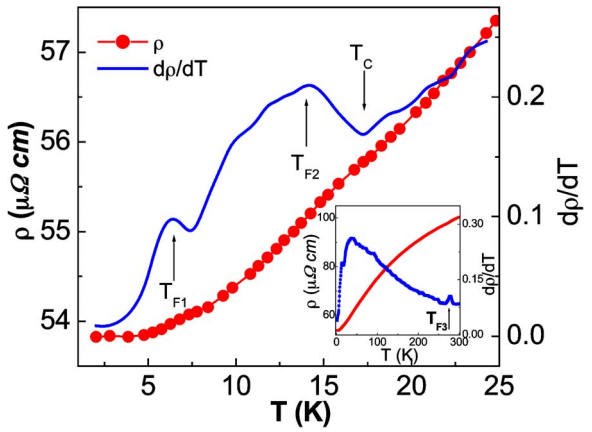

FIG. 6. (Color online) Temperature dependence of the electrical resistivity ρ (left axis) and its derivative $d\rho/dT$ (right axis), the insert shows the details in temperature ranging from 2 K to 300 K.

periodic long-range magnetic order is one of the defining properties of a SG system.[1,12] However, a detailed inspection of the derivative of $\rho(T)$ with respect to T reveals clearly three broad and well-shaped maxima around $T_{F1}\approx 6.5$ K, $T_{F2}\approx 14$ K, and $T_{F3}\approx 275$ K (the very broad peak around 40 K is related to the characteristic structure of the BMG), they are very close to the freezing temperatures defined by the cusps in the magnetic susceptibility. The resistance maximum is attributed to the exchange interaction between conduction electrons and localized spins,[20] suggesting that some sort of weak spin ordering changes, which are in good agreement with the presence of spin freezing phenomena around T_{F1}, T_{F2}, and T_{F3} inferred from ac and dc magnetizations. This electronic transport property excludes the existence of long-range spatial magnetic ordering at T_{F1}, T_{F2}, and T_{F3}, and further confirms the multiple-SGL behaviors in the BMG.

The multiple SGL behaviors are also supported by magnetic relaxation experiments. To picture the complete dynamics of the multiple SGL freezing at different temperatures, the T dependence of thermoremanent magnetization (TRM) was performed as follows: The sample was first cooled down from 300 to 2 K in a strong field of 90 kOe; at 2 K, the field was removed and the remanence was measured with increasing temperature up to 300 K. It is known that a SG system is not in thermal equilibrium but slowly relaxes to lower energy states, which can be characterized by the stretched exponential, logarithmic or power laws.[11,18] We fit the TRM data with a power law:[10,11] $M_{TRM}\propto T^{-\beta}$, the slope changes of the log-log plot of TRM vs T exhibit two broad decay regions around T_{F2}, and T_{F3} (see Fig. 7). Below the freezing temperature T_F, the TRM is roughly consistent with the power decay law, while TRM decreases faster when $T>T_F$, implying that the thermal activated process slowly reduces the glassy behavior exhibited below T_F in comparison with the fast decay above T_F. Furthermore, the TRM shows a decrease at whole measured T range and a magnetic phase

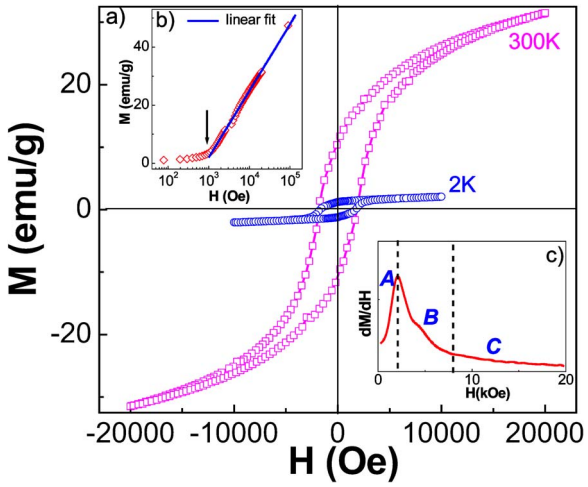

FIG. 8. (Color online) (a) The *M-H* hysteresis loops at 300 K and 2 K after zero-field-cooled. (b) the initial magnetization curve at 2 K, the solid line shows the linear fit. (c) The dM/dH vs applied field at 2 K.

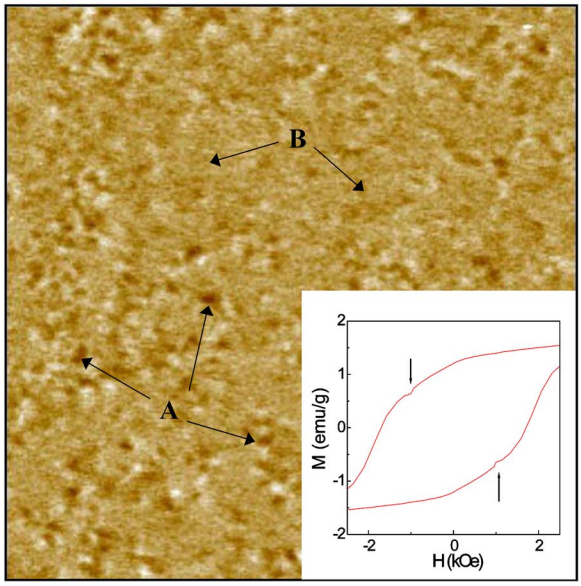

FIG. 9. (Color online) The typical (10×10 μm) MFM image of the BMG, the regions marked by *A* denote the magnetic domain structures with random distribution, and the large gray areas (nonferromagnetic) are indicated by marker *B*. The insert shows the enlarged *M-H* hysteresis loop at 300 K, the arrows show weak steplike feature.

transition around 17 K, where the ac susceptibility show no frequency dependence and no irreversibility between ZFC and FC modes. The PM-to-FM transition is so strong that should originate from the paramagnetic amorphous matrix with a large volume fraction in the BMG. In addition, the nonzero value 1.2 emu/g of TRM at 300 K is the same with the remanent magnetization M_r measured by the hysteresis loop, confirming there exist ferromagnetic nanoclusters with short-range interacting embedded in paramagnetic amorphous matrix.[10] The time response of dc magnetization is also important to reveal the spin dynamics for SG system. The isothermal remanent magnetization (IRM) was measured as follows: the sample was firstly cooled down in zero field from 300 K to 3 K, and a magnetic field $H=500$ Oe was applied for 1000 s, then the field was removed and the remanence was measured as a function of time. As shown on the semilogarithmic plot in the insert of the Fig. 7, the IRM can be roughly fit by a power law:[10,11] $M_{IRM}\propto t^{-\beta}$, the sight deviation may be related to the coexistence of multiple SGL freezing states.

Figure 8(a) presents the *M-H* hysteresis loops at 300 K and 2 K after ZFC. The BMG shows a hard magnetic property and no obvious hysteresis shift, and the coercivity (146 kA m^{-1}) is almost the same at 300 and 2 K, but the ratio between remanent and saturation magnetizations (M_r/M_s) decreases from 0.59 at 300 K to 0.33 at 2 K. The initial magnetization M_i curve at 2 K is plotted as a semilogarithmic scale in Fig. 8(b), the solid line shows the linear fit. It is worth noting that the magnetization is difficult to saturated even in a high magnetic field up to 90 kOe, favoring to the representative SG effect.[5,6] The M_i increases slowly below 1 kOe, but the linear increase above 1 kOe follows the power law, which characterizes the SGL freezing nature of the system.[11,18] More detail is shown by the derivative of M_i at 2 K [see Fig. 8(c)], from the slope's changes, there exist three regions (denoted by *A*, *B*, and *C*) separated by two kinks around 2 kOe and 8 kOe. With increasing field, the dM/dH increases rapidly in region *A* according to the ferromagnetic nanoclusters ordering under applied field, while decreases slowly in regions *B* and *C*. The second kink around 8 kOe between regions *B* and *C* is very close to the critical cooling field $H_{cri}\approx8.2$ kOe calculated by the forenamed AT line, further confirming that the reentrant SGL at $T_{F2}\approx14$ K may disappear when $H>H_{cri}$.

To understand the microstructural origin of the observed multiple-SGL behaviors in the BMG, the magnetic force microscope (MFM) is performed on the BMG at RT. The typical (10×10 μm) MFM image is presented in Fig. 9. Some magnetic domain regions with obvious magnetic contrast (denoted by *A*) in large gray areas (the nonferromagnetic regions denoted by *B*) are visible, and the average domain width is ~180 nm, which is similar to that of other hard magnetic BMGs.[21] The MFM image implies that the ferromagnetic clusters in a small volume fraction coexist with paramagnetic amorphous matrix in the BMG. However, the BMG exhibits a typical amorphous XRD pattern, which gives an upper limit of a few nanometers for the cluster size. The average domain width is much larger than the cluster size because of the exchange-coupling interaction in the alloy,[21] i.e., the domain is actually a collection of a group of the nanoclusters with similar magnetic orientations aligned by exchange coupling. Partial nanoclusters have been identified as Pr and Pr-Fe phases, and the nanoclusters with size of nearly 2 nm in rare earth (RE)-based magnetic BMGs have been directly observed by transmission electron microscopy.[22] The MFM image indicates the Pr-based BMG has an intrinsic inhomogeneous microstructure consisting of amorphous matrix and magnetic nanoclusters.

The inset of Fig. 9 shows the enlarged *M-H* hysteresis loop at 300 K, the arrows show two weak kinks at 1 kOe, indicating a two-phase behavior,[23] which nicely coincides

with the two kinds of magnetic domains observed by MFM. For the optimal effective exchange coupling to occur within a two-phase magnet, the dimension of the soft phase should be smaller than twice the domain wall width of the hard phase.[23] Therefore, in a BMG with a very large soft phase, hard and soft phases are not able to switch corporately. As a result, its hysteresis loop shows a two-phase behavior and the kink is related to the magnetization reversal of the ferromagnetic nanoclusters. According to the strong pinning model,[24] the ferromagnetic nanoclusters may act as pinning sites for the domain walls of the amorphous matrix, the constant coercivity at 300 K and 2 K suggests that these ferromagnetic nanoclusters remain stable in low T. Taking account of the initial magnetization kink at 2 K nearly in the same low field range [see Figs 8(b) and 8(c)], the behaviors are in good accordance with the cluster-SGL freezing process near RT.

IV. DISCUSSIONS

We ascribe the unusual multiple SGL behaviors to the intrinsic inhomogeneous microstructure of the Pr-based BMG. The BMG contains ferromagnetic Fe or Ni containing nanoclusters, paramagnetic Pr-based amorphous matrix and Pr nanoclusters, which contribute to the cluster-SGL at $T_{F3} \approx 280$ K, the reentrant-SGL at $T_{F2} \approx 14$ K, and the cluster-SGL at $T_{F1} \approx 6$ K, respectively (T_F is identified by the ac magnetic susceptibility). It is worth noting that the SGL temperatures estimated by different kinds of measurements are slightly different, their magnitudes are within the realm of conventional SG phase. A larger negative heat of mixing of the constituents, ΔH_{mix} is necessary to stabilize bulk metallic glass. However, for the Pr-based BMG, the ΔH_{mix} between the two components (Pr and Fe) is positive and hence liquid is to be less stable, consequently the mutually repulsive interaction between Pr and Fe leads to clustering in the supercooled liquid, the clustering in the liquid state will be frozen and retained in the amorphous Pr-based alloy.[25] The initial nanoscale nucleation may be responsible for the intrinsic inhomogeneous microstructure of Pr-based BMG. In fact, the precipitation of magnetic nanoclusters has been found to be a common phenomenon for rare earth (RE)-Fe based glass-forming alloy.[22]

The detail mechanism for the multiple SGL behaviors in the Pr-based BMG is not understandable yet. It needs further studies to verify the three SGL transitions are true SGs or not. SG is an example of spontaneous cooperative freezing of the spin orientations in the presence of the constrained disorder of the interactions or spin locations, which are generally associated with large degeneracy of the magnetic states caused by disorder, frustration, or both.[1,8] The total freezing process of multiple SGL behaviors can be qualitatively speculated as follows: The ferromagnetic Fe or Ni containing nanoclusters are well confined in the amorphous matrix during high-rate cooling process, and the large-area magnetic domain near RT indicates these nanoclusters are ferromagnetically coupled by exchange interaction. The orientation of the nanoclusters depends on the competition between the exchange coupling energy and the magnetocrystalline anisotropy. If these interactions are strong enough in RT, accompanying with the frustration of the magnetic completing, the ferromagnetic nanoclusters will turn into a collective dynamical behavior (i.e., the observed weak cluster-SGL).[7,26] With deceasing temperature, as the paramagnetic Pr-based amorphous matrix becomes ferromagnetic below $T_C \approx 17$ K, the spontaneous ferromagnetic order starts. The absence of strong susceptibility divergence from the Curie-Weiss law below T_C suggests that ferromagnetic amorphous matrix do not represent the true long-range ordered ferromagnetic domains.[10] With further cooling below $T_{F2} \approx 14$ K, the atomic disorder and site disorder of the magnetic elements may provide magnetic competition between FM and AFM interactions (the Pr-Fe and Fe-Fe interactions are ferromagnetic, while the antiparallelly coupled Pr-Pr moments are antiferromagnetic). And the magnetic RKKY competition cannot be ruled out, but its contribution should be secondary in view of the strong ferromagnetism starting below 17 K (see Fig. 7).[27] Thus no unique spin configuration is favored in this case, leading to the frustration of amorphous matrix and the subsequent spin freezing process.[1] The AFM ordering temperature resulting from RE-RE interactions has been clearly observed below 20 K in by neutron-diffraction measurements, which is very weak in RE-Fe based metallic glasses and difficult to be definitely confirmed by conventional magnetic measurements.[28]

In addition to ferromagnetic Fe or Ni containing nanoclusters, it is worth noting that there also exit a small fraction of paramagnetic Pr nanoclusters well confined in the amorphous matrix.[22] With deceasing temperature, the Pr nanoclusters becomes ferromagnetic below T_C, the ferromagnetic spin order is established within each Pr nanocluster and the growth of the ferromagnetic spin-correlation length is enhanced by intercluster interactions. The freezing of Pr nanoclusters needs a lower temperature than that of amorphous matrix, because of the longer ferromagnetic spin-correlation length extending over nanoclusters. Below T_{F1}, the spin directions of these ferromagnetic Pr nanoclusters are frozen owing to frustrated intercluster interactions, which play an dominant role in determining a weak cluster-SGL ordering around $T_{F1} \approx 6$ K. However, for canonical cluster-SG, the slope change of TRM at the freezing temperature is rather weak,[10,11] the Pr cluster-SGL ordering around $T_{F1} \approx 6$ K may be too weak to be observed in TRM due to the very small fraction of Pr nanoclusters and weak intercluster interactions. Similarly, a small shoulder at a temperature slightly lower than the main freezing peak temperature has also been reported in a typical ferromagnetic cluster glass U_2IrSi_3,[12] which has been ascribed to an inhomogeneous magnetic structure existing in the sample to a certain extent. A hierarchical SGL ordering can also be another possible mechanism for the transition at 6 K. In other words, although the transition at 6 K is in accord with some basic characteristics of SG system, it may not be a canonical SGL transition (the detail study is in process).

V. CONCLUSIONS

The unusual multiple SGL behaviors including a reentrant-SGL and two cluster SGL, have been observed in

the $Pr_{60}Al_{10}Ni_{10}Cu_{16}Fe_4$ BMG. The cluster SGL at 6 K, reentrant SGL at 14 K, and cluster SGL near RT originate from the Pr nanoclusters, amorphous matrix and ferromagnetic Fe or Ni containing nanoclusters, respectively. The multiple SGL behaviors are ascribed to the cooperation of the intrinsic inhomogeneity, the spontaneous nanoscale confinement and completing magnetic interactions in the BMG. The Pr-based BMG with three different SGL phases not only facilitates the untouched researches for the interactions between two or more SGs, but also provides an ideal prototype for more complex systems, which has both fundamental and applied significance. In addition, the inhomogeneous microstructure can be easily tuned by introducing magnetic elements such as Fe in various RE-based BMGs, therefore, a variety of multiple SGL behaviors can be realized in these RE-based BMGs.

ACKNOWLEDGMENT

The support of the Natural Science Foundation of China (Contracts No. 50321101 and No. 50225101) is appreciated.

*Author to whom correspondence should be addressed.
Electronic address: whw@aphy.iphy.ac.cn

[1] K. Binder and A. P. Young, Rev. Mod. Phys. **58**, 801 (1986).
[2] T. Taniguchi, K. Yamanaka, H. Sumioka, T. Yamazaki, Y. Tabata, and S. Kawarazaki, Phys. Rev. Lett. **93**, 246605 (2004).
[3] N. Sourlas, Nature (London) **339**, 693 (1989).
[4] R. H. Kodama, A. E. Berkowitz, E. J. McNiff, Jr., and S. Foner, Phys. Rev. Lett. **77**, 394 (1996); T. Zhu, B. G. Shen, J. R. Sun, H. W. Zhao, and W. S. Zhan, Appl. Phys. Lett. **78**, 3863 (2001).
[5] B. Martinez, X. Obradors, Ll. Balcells, A. Rouanet, and C. Monty, Phys. Rev. Lett. **80**, 181 (1998).
[6] H. Wang, T. Zhu, K. Zhao, W. N. Wang, C. S. Wang, Y. J. Wang, and W. S. Zhan, Phys. Rev. B **70**, 092409 (2004).
[7] E. Bonetti, L. Del Bianco, D. Fiorani, D. Rinaldi, R. Caciuffo, and A. Hernando, Phys. Rev. Lett. **83**, 2829 (1999).
[8] W. Bao, S. Raymond, S. M. Shapiro, K. Motoya, B. Fak, and R. W. Erwin, Phys. Rev. Lett. **82**, 4711 (1999).
[9] J. Dho, W. S. Kim, and N. H. Hur, Phys. Rev. Lett. **89**, 027202 (2002).
[10] R. N. Bhowmik and R. Ranganathan, J. Appl. Phys. **93**, 2780 (2003).
[11] R. N. Bhowmik and R. Ranganathan, J. Magn. Magn. Mater. **237**, 27 (2001); **248**, 101 (2002).
[12] D. X. Li, S. Nimori, Y. Shiokawa, Y. Haga, E. Yamamoto, and Y. Onuki, Phys. Rev. B **68**, 172405 (2003).
[13] M. Mezard, G. Parisi and M. Virasoro, Spin Glass Theory and Beyond: *An Introduction to the Replica Method and Its Applications* (World Scientific, Singapore, 1987).
[14] Y. Muraoka, H. Tabata, and T. Kawai, Appl. Phys. Lett. **77**, 4016 (2000).
[15] J. J. Kim, Y. Choi, S. Suresh, and A. S. Argon, Science **295**, 654 (2002).
[16] W. H. Wang, C. Dong, and C. H. Shek, Mater. Sci. Eng., R. **44**, 45 (2004).
[17] Z. F. Zhao, D. Q. Zhao, and W. H. Wang, Appl. Phys. Lett. **82**, 4699 (2003).
[18] S. D. Tiwari and K. P. Rajeev, Phys. Rev. B **72**, 104433 (2005).
[19] H. Maletta and W. Zinn, in *Handbook on the Physics and chemistry of Rare Earths*, edited by K. A. Gschneidner, Jr. and L. Eyring (North-Holland, Amsterdam, 1989), Vol. 12, Chap. 84; J. R. L. de Almeida and D. J. Thouless, J. Phys. A **11**, 983 (1978).
[20] U. Larsen, Phys. Rev. B **14**, 4356 (1976).
[21] B. C. Wei, W. H. Wang, M. X. Pan, B. S. Han, Z. R. Zhang, and W. R. Hu, Phys. Rev. B **64**, 012406 (2001).
[22] Y. T. Wang and W. H. Wang, J. Non-Cryst. Solids **352**, 444 (2006); A. Inoue, A. Takeuchi, and T. Zhang, Metall. Mater. Trans. A **29A**, 1779 (1996); G. J. Fan, W. Löser, J. Eckert, and L. Schultz, Appl. Phys. Lett. **75**, 2948 (1999).
[23] H. Zeng, J. Li, J. P. Liu, Z. L. Wang, and S. H. Sun, Nature (London) **420**, 395 (2002).
[24] R. S. Turtelli, D. Triyono, R. Grossinger, H. Michor, J. H. Espina, J. P. Sinnecker, H. Sassik, J. Eckert, G. Kumar, Z. G. Sun, and G. J. Fan, Phys. Rev. B **66**, 054441 (2002).
[25] B. S. Murty and K. Hono, Appl. Phys. Lett. **84**, 1674 (2004); Z. G. Sun, W. Löser, J. Eckert, K.-H. Müller, and L. Schultz, *ibid.* **80**, 772 (2002).
[26] J. L. Dormann, F. D'Orazio, F. Lucari, E. Tronc, P. Prene, J. P. Jolivet, D. Fiorani, R. Cherkaoui, and M. Nogues, Phys. Rev. B **53**, 14291 (1996); H. Mamiya, I. Nakatani, and T. Furubayashi, Phys. Rev. Lett. **80**, 177 (1998); T. Jonsson, P. Svedlindh, and M. F. Hansen, Phys. Rev. Lett. **81**, 3976 (1998).
[27] J. A. De Toro, M. A. Lopez delaTorre, J. M. Riveiro, R. SaezPuche, A. Gomez-Herrero, and L. C. Otero-Diaz, Phys. Rev. B **60**, 12918 (1999); D. X. Li, K. Sumiyama, K. Suzuki, and T. Suzuki, *ibid.* **55**, 6467 (1997).
[28] R. S. Turtelli, D. Triyono, R. Grossinger, H. Michor, J. H. Espina, J. P. Sinnecker, H. Sassik, J. Eckert, G. Kumar, Z. G. Sun, and G. J. Fan, Phys. Rev. B **66**, 054441 (2002).